

**IMECE2006-13764**

## **RESIDUAL STRESS VARIATION IN POLYSILICON THIN FILMS**

**Andrew J. Mueller and Robert. D. White**

Mechanical Engineering, Tufts University, Medford, MA 02155

### **ABSTRACT**

This paper compares the use of four mechanical methods for characterization of residual stress variation in low pressure chemical vapor deposited (LPCVD) polysilicon thin films deposited, doped, and annealed under different conditions. Stress was determined using buckling structures, vibrating microstructures, static rotating structures and the wafer curvature method. After deposition of 1.0  $\mu\text{m}$  of polysilicon at 625°C and 588°C the stress in the wafers is 230 MPa compressive (stdev = 1.2 MPa) and 340 MPa compressive (stdev = 10.4 MPa), respectively. Deposition of 0.6  $\mu\text{m}$  at 580°C results in a tensile stress of 66 MPa (stdev= 52 MPa). Following doping, all stresses are compressive. Boron doping of the 625°C and 588°C deposited films produces a compressive stress of 149 MPa (stdev= 28.6 MPa) and 100 MPa (stdev= 29.5 MPa). Phosphorous doping of the 588°C and 580°C deposited films produces a compressive stress of 54 MPa (stdev = 0.3 MPa) and 80 MPa (stdev= 5.3 MPa), respectively. Annealing through rapid thermal processing (RTP) at temperatures of 1000°C – 1100°C reduced the stresses by 20-50 MPa, but the stresses remained compressive. These values are measured using the wafer curvature method. Values obtained from the other microstructure methods agree with stresses determined by wafer curvature with the exception of the rotating structures which showed 20% lower stress readings.

### **INTRODUCTION**

Polycrystalline silicon (polysilicon) is a valuable material in microelectromechanical systems (MEMS) due to its versatility. It can be used as a mechanical or sacrificial layer in both sensor and actuator applications and can exhibit a wide range of mechanical properties depending on how it is processed. It is important to characterize these mechanical properties for better process development and monitoring, as well as from a

reliability and performance standpoint. Residual stress in particular is important to understand, especially when dealing with thin films. Compressive stresses may initiate film buckling while highly tensile stresses can result in film cracking. Even when stresses do not cause catastrophic failure, they seriously impact device performance. For most applications a film with low tensile stress or no stress at all is desired.

Some measurements of the residual stress in LPCVD polysilicon films and the influence of doping and annealing on film stress have been reported [1, 2, 3]. Stress variations across processes as well as stress variation through the polysilicon film thickness (out-of-plane) were looked at. Results indicate that as-deposited, undoped polysilicon is not suitable for MEMS applications due to the high residual stress present after deposition. This stress depends largely on deposition temperature and pressure and ranges from ~400 MPa tensile to ~400 MPa compressive over a relatively small temperature change (580°C to 630°C), shifting drastically from highly compressive to highly tensile and back to highly compressive stress within these temperatures. Subsequent annealing (at temperatures  $\geq 1000^\circ\text{C}$  with rapid thermal processing (RTP) or furnace annealing) or doping (using boron or phosphorous) can reduce the residual stress to low compressive or tensile values [1, 2, 3].

Because of the importance of residual stresses in thin film processing, accurate and straightforward techniques for local stress determination are desired. Characterizing stress variations both across single wafers as well as across different processes is critical in order to properly design structures. In the past 20 years many mechanical methods have been developed for determining stress variation in thin films [4,5]. In this paper four of these methods are compared using LPCVD polysilicon films. The elastic modulus of the thin film is determined first using cantilevered beam resonance. Stress is then determined using buckling structures, vibrating microstructures, static rotating structures and the wafer curvature method. Attention is

paid to the variation of stress across single wafers as well as across different deposition processes.

## THEORY

Cantilevered beams are used to determine elastic modulus of the polysilicon through use of the resonant frequency of the beams,

$$f_1 = 0.56 \sqrt{\frac{Eh^2}{12\rho L^4}} \quad (1)$$

where  $f_1$  is the resonant frequency of the beams,  $E$  is the elastic modulus,  $h$  is the beam thickness,  $\rho$  is the density of the polysilicon, and  $L$  is the beam length [6]. An array of 17 cantilevered beams is used to determine the elastic modulus of the polysilicon.

Doubly clamped beams are also used, both as a buckling beam array and as a vibrating microstructure array. Using the beam array for the buckling beam method, the stress in the beams is related to the critical length ( $L_c$ ) where buckling occurs through the use of Euler's equation for elastic instability of struts,

$$\sigma = E \left( \frac{4\pi^2 I}{AL_c^2} \right) \quad (2)$$

where  $A$  is the cross-sectional area of the beam and  $I$  is the area moment of inertia, and  $\sigma$  is the stress in the beam [7, 8].

Using the doubly clamped beams as vibrating microstructures, the resonant frequencies of the beams are related to the residual stress as well. The resonant frequency of a double clamped beam with a rectangular cross section can be found through the differential equation for beam deflection  $w$  as a function of distance  $x$  along the beam and time  $t$  is given by,

$$EI \frac{\partial^4 w}{\partial x^4} - \sigma A \frac{\partial^2 w}{\partial x^2} + \rho A \frac{\partial^2 w}{\partial t^2} = 0 \quad (3)$$

where  $\sigma$  is the stress in the beam [8,9]. Following the work of Guckel *et al.* [9], an approximate analytical solution for equation 3 is found using Rayleigh's method,

$$\omega_{est}^2 = \frac{\int_0^L EI \left( \frac{d^2 W(x)}{dx^2} \right)^2 dx + \sigma A \int_0^L \left( \frac{dW(x)}{dx} \right)^2 dx}{\int_0^L \rho A W^2(x) dx} \quad (4)$$

where  $W$  is an estimation of the first mode shape and integration is carried out over the entire length,  $L$ , of the beam. The deflection profile of a doubly clamped beam under a uniformly distributed load is chosen for an estimation of the first mode shape and results in the following expression for  $\omega_{est}$ ,

$$\omega_{est}^2 = \left( \frac{504EI}{L^4 \rho A} \right) \left( 1 + \frac{\sigma AL^2}{42EI} \right) \quad (5)$$

Using equations 2 and 5, the residual stress in the polysilicon is determined by recording at which lengths the doubly clamped beams buckle and by recording the resonant frequencies of the beams, respectively. Results are given below.

Micro-rotating structures differ from both the buckling and resonating structure methods in that there is a linear relationship between residual stress and observed tip deflection, which can be seen simply by use of an optical microscope. Using finite element methods (FEM), Zhang *et al.* [10] determine the relationship between deflection and stress.

The rotational deflection ( $\delta_{tip}$ ) of the rotating beams is determined by a vernier scale and can be related to the stress in the beams through the following expression provided by Zhang:

$$\sigma = \frac{E \delta_{tip}}{\alpha f_0} \quad (6)$$

where  $\alpha$  is the length correction coefficient and  $f_0$  is the sensitivity factor for the design. These values are tabulated in [10]. For the structure used  $\alpha$  is 1 and  $f_0$  is 6.49  $\mu\text{m}$ .

## PROCESSING

The 0.6  $\mu\text{m}$  and 1.0  $\mu\text{m}$  thick films characterized were deposited, doped, and annealed under different conditions. Deposition occurred at temperatures of 580°C (110 mT, 80 sccm SiH<sub>4</sub>), 588°C (110 mT, 80 sccm SiH<sub>4</sub>), or 625°C (120 mT, 80 sccm SiH<sub>4</sub>). For the lower temperature depositions (below 600°C), the amorphous layer initially surrounding the silicon grains was crystallized during the doping process to form a polycrystalline structure with larger grains. For films deposited at 625°C, grain boundaries were already formed and

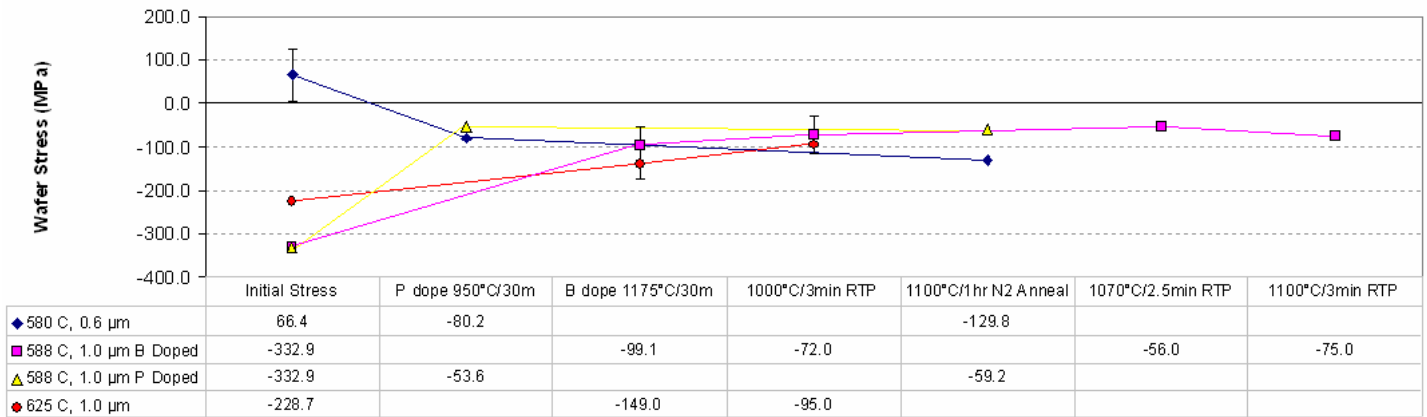


FIGURE 1. SUMMARY OF RESIDUAL STRESS VARIATION ACROSS WAFER PROCESSES.

the polycrystalline structure characteristic of polysilicon was established before doping [11]. The thin films were doped with boron (using solid source diffusion for 30 minutes at 1175°C) or phosphorous (using gas phase  $\text{POCl}_3$  for 30 minutes at 950°C).

Test structures for the vibrating microstructures, static rotating structures, and buckling beams were microfabricated in four of the polysilicon thin films processed. To etch through the polysilicon into the underlying sacrificial oxide layer reactive ion etching was performed using  $\text{SF}_6$  (50 sccm) and  $\text{O}_2$  (5 sccm) at 30 mTorr pressure and 400 W power. The oxide was subsequently etched away in concentrated (49%) HF, undercutting and releasing the polysilicon structures. The structures were rinsed in methanol prior to drying to reduce stiction. The subsequent use of critical point drying would further reduce stiction but was not employed.

## RESULTS AND DISCUSSION

Wafer curvature measurements are produced using the KLA-Tencor Flexus 2320 and the resulting stress values are compared to the remaining three methods. Using stress values obtained from the wafer curvature method, Figure 1 compares the residual stresses across the different processes analyzed. The stress after deposition is found to be 229 MPa compressive (stdev = 1.2 MPa) for a 1.0 μm film deposited at 625°C, 333 MPa compressive (stdev = 10.4 MPa) for a 1.0 μm film deposited at 588°C, and 66 MPa tensile (stdev= 52 MPa) for a 0.6 μm film deposited at 580°C. While the change in initial stress between the films deposited at 580°C and 588°C agrees with results from other authors, as discussed above, the reason for the drastic shift from tensile to compressive stress is not fully understood [2, 12].

Boron doping of the 625°C and 588°C deposited films produces compressive stresses of 149 MPa (stdev= 28.6 MPa) and 100 MPa (stdev= 29.5 MPa) respectively. Phosphorous doping of the 588°C and 580°C deposited films

produces compressive stresses of 54 MPa (stdev = 0.3 MPa) and 80 MPa (stdev= 5.3 MPa) respectively. Annealing through RTP at temperatures of 1000 – 1100°C completed after doping reduces the stresses by 20-50 MPa, but in all cases the film stresses remain compressive. This result differs from results obtained by other authors who annealed their films using RTP *prior* to doping, producing tensile films [13].

Stress variations across single wafers is obtained through analysis of the following four wafers containing microstructures: two wafers with 1 μm thick films deposited at 588°C, one with phosphorous doping, designated wafer “A”, the other with boron doping, designated wafer “B”; one wafer with a boron doped 1 μm thick film deposited at 625°C, designated wafer “C”; and one wafer with a phosphorous doped 0.6 μm thick film deposited at 580°C, designated wafer “D”. None of the wafers with microstructures underwent RTP. Figure 2 shows the wafer curvature maps for all 4 wafers. As shown in the figure, stress variation across the wafers is as large as 80 MPa.

Microstructures were fabricated on all four wafers. However, due to problems with stiction after processing, only wafer A yielded enough data to show single wafer stress variation obtained from microstructures. This is likely due to the fact that wafer A has the lowest average residual stress and the thicker of the two films deposited. Even so, stiction remains an issue for the analysis of wafer A and limits the data available. The affects of stiction can be seen in Figure 3 where the three longest cantilevered beams (70, 80, and 90 μm) are stuck down. All further analysis is conducted on this wafer. Figure 2 shows the wafer curvature map for wafer A and details the approximate location of test structures.

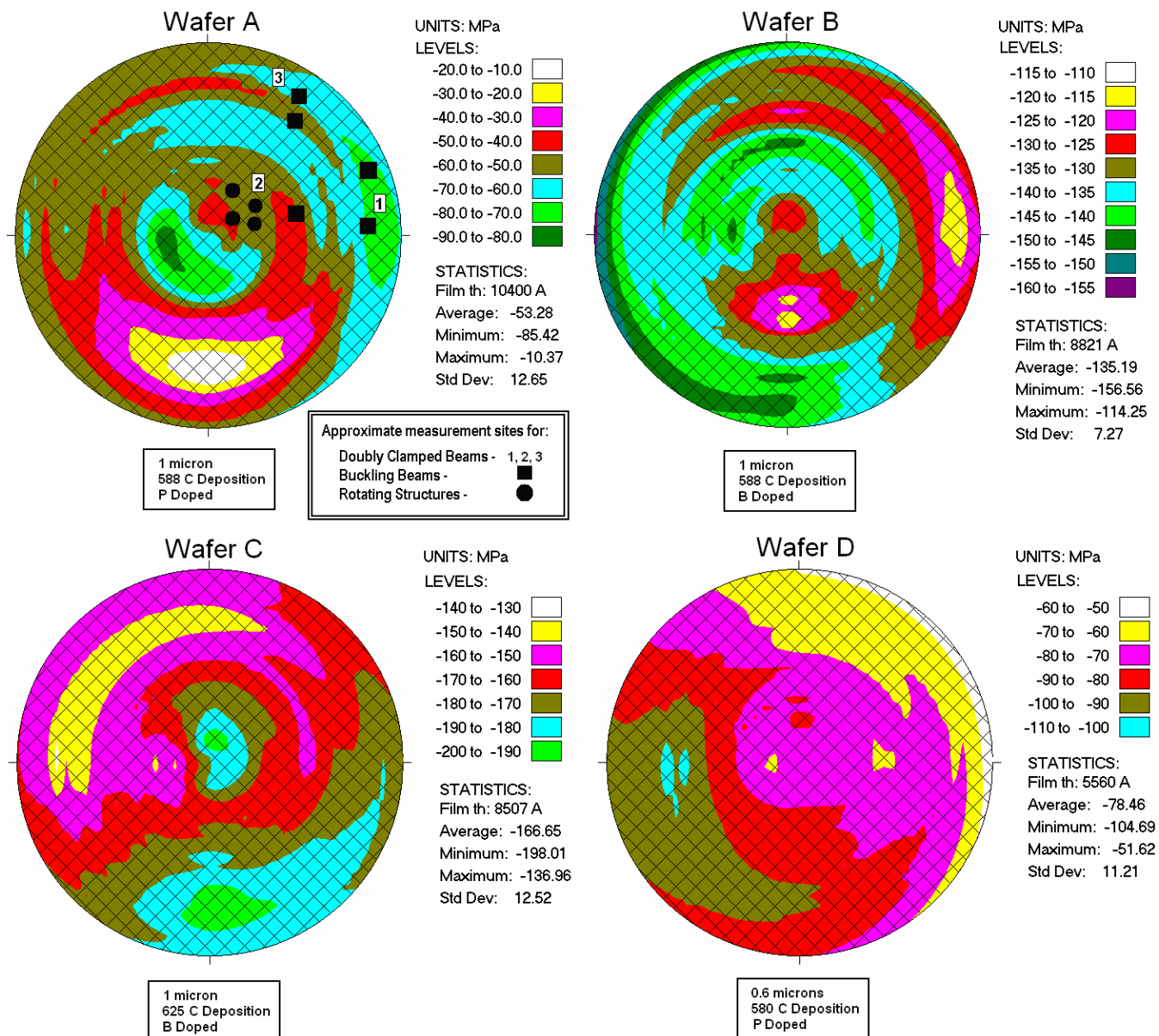


**FIGURE 2. WAFER CURVATURE MAPS FROM ALL WAFERS CONTAINING MICROFABRICATED STRUCTURES. APPROXIMATE MICROSTRUCTURE LOCATIONS FOR WAFER A ARE SHOWN.**

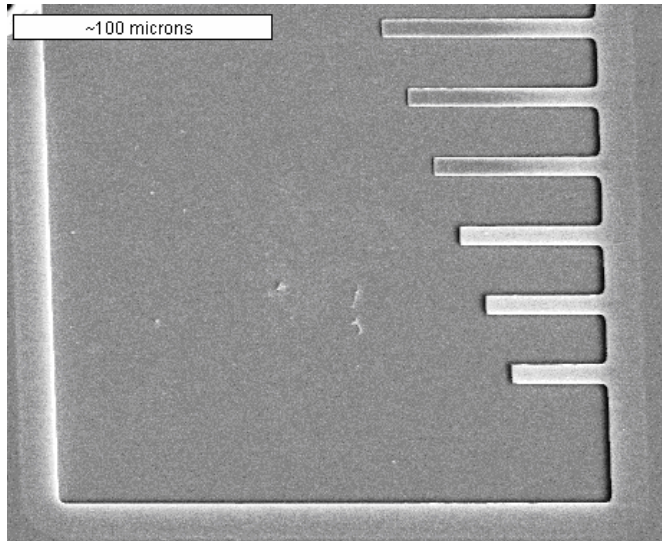
### Cantilevered Beams

Figure 3 partially shows the cantilevered beam array used to determine the elastic modulus of the film. The array varies in length from 40 to 200  $\mu\text{m}$  in increments of 10  $\mu\text{m}$ . Resonant frequencies of both cantilevered and doubly clamped beam arrays are measured using laser vibrometry during electrostatic actuation. A low frequency square wave is applied to the beams, exciting a step response and allowing the beams to resonate at their damped natural frequencies which are then recorded through laser vibrometry.

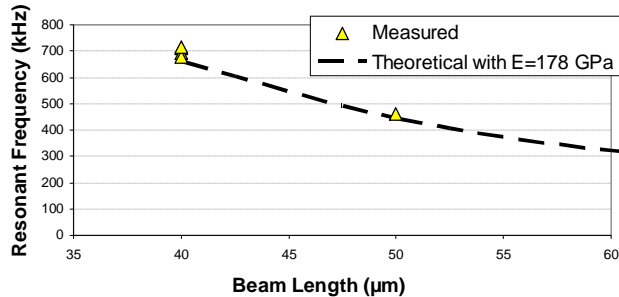
Before analysis is conducted on either the cantilevered or doubly clamped beams, length correction

factors are added on to beam lengths due to the undercutting that occurs during device. An undercutting of 15  $\mu\text{m}$  occurs at the ends of both types of beams creating a shelf that resonates with the beams. This undercutting can be seen in Figures 3 and 5. Length corrections of 6  $\mu\text{m}$  for cantilevered, and 21  $\mu\text{m}$  for doubly clamped beams, must be added onto the actual beam length to properly calculate the elastic modulus and residual stress. Length corrections are obtained by determining the length that, when added to actual beam lengths, minimizes standard deviations in the elastic modulus calculated from beam resonant frequencies measured at a single die. The lengths are confirmed using FEM analysis by matching frequencies obtained from FEM beams, undercut by

15  $\mu\text{m}$ , with calculated frequencies of beams using their effective lengths. Figure 4 shows the observed resonant frequencies of cantilevered beams against the theoretical frequencies using effective lengths. Resonant frequencies indicate an elastic modulus of  $E=178 \text{ GPa}$  (stdev = 7.6 GPa) which is used with the three methods below to determine the residual stress in the thin film. Although stress variation in the out of plane direction was not tested during this work, curling in cantilevered beams was not observed and the affect of this stress on devices is assumed to be minimal.



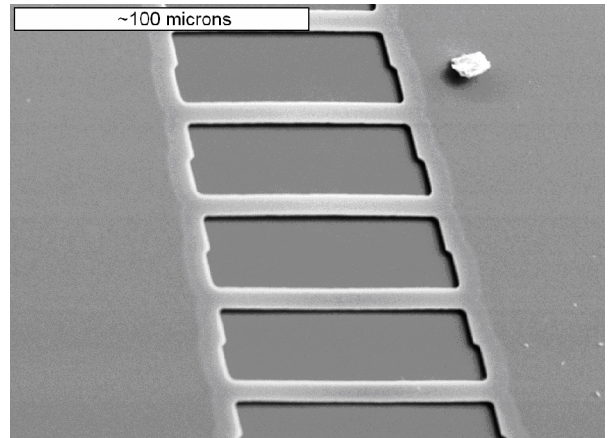
**FIGURE 3. SEM IMAGE OF CANTILEVER BEAM ARRAY.**



**FIGURE 4. RESONANT FREQUENCIES OF THE CANTILEVERED BEAM ARRAY COMPARED TO THEORETICAL VALUES FOR  $E=178 \text{ GPa}$ .**

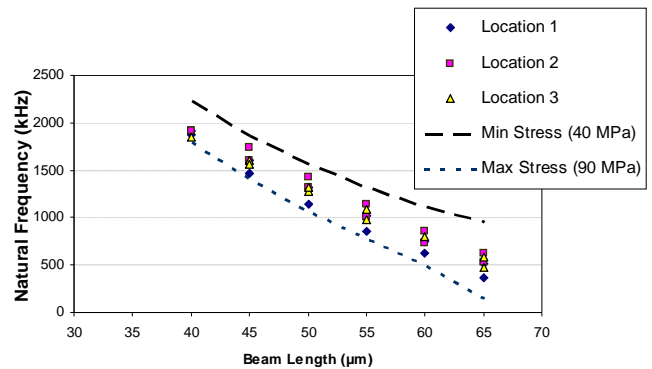
### Doubly Clamped Beams

Figure 5 shows a doubly clamped beam array analyzed on wafer A. The arrays include 32 beams from 40 to 600  $\mu\text{m}$  in length, varying in increments of 5  $\mu\text{m}$  for the first 27 beams and 100  $\mu\text{m}$  for the last 5.



**FIGURE 5. SEM IMAGE OF DOUBLY CLAMPED BEAM ARRAY. ABOUT 15  $\mu\text{m}$  OF UNDERCUTTING IS VISIBLE.**

A Wyko non-contact profiler is used to determine buckling lengths of the doubly clamped beams. Figure 6 shows the resonant frequency vs. length curve for three array locations. Beam resonant frequencies are compared to frequencies calculated from the wafer curvature method's estimated maximum and minimum stress at corresponding locations (see Figure 2). Four beams of lengths between 40 and 65  $\mu\text{m}$  are measured at each location. As shown, the residual stresses obtained from this method vary between 50 and 90 MPa compressive (stdev= 4.8 MPa) and correspond to values given by the wafer curvature method.



**FIGURE 6. RESONANT FREQUENCIES FOR DOUBLE CLAMPED BEAMS ON WAFER A FOR LOCATIONS 1, 2 AND 3 (SEE FIGURE 2). THEORETICAL CURVES ARE GIVEN FOR 50 MPa AND 90 MPa COMPRESSIVE STRESSES.**

Buckling lengths of the doubly clamped beam arrays are observed from 70 to 80  $\mu\text{m}$ . Stresses indicated by these buckling lengths are also within the range determined by wafer curvature, varying between 50 and 70 MPa compressive.

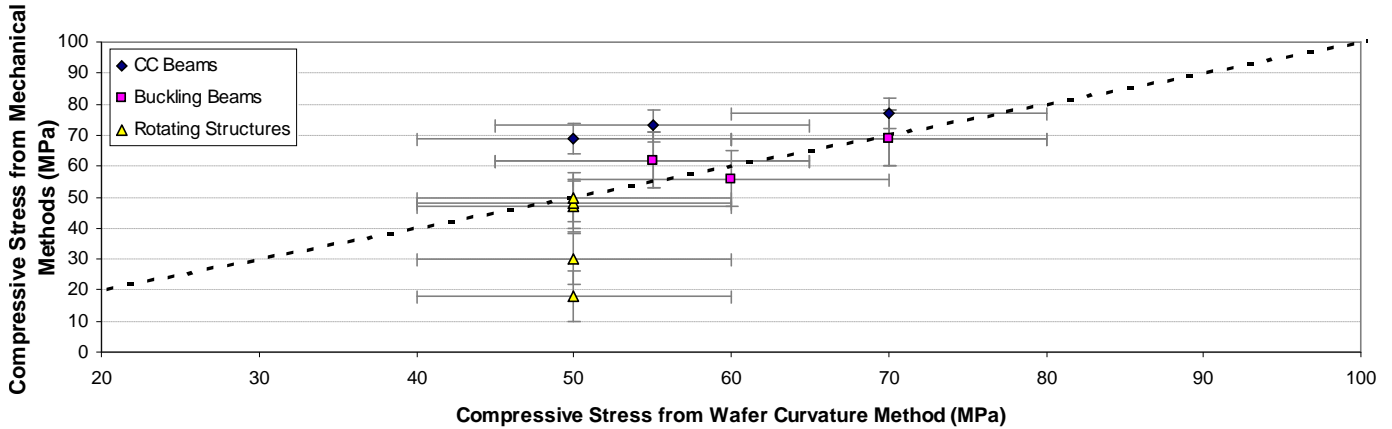


**FIGURE 7. COMPARISON OF STRESS MEASUREMENT RESULTS BETWEEN MICROFABRICATED STRUCTURES AND THE WAFER CURVATURE METHOD. THE DASHED LINE INDICATES COMPLETE AGREEMENT BETWEEN METHODS.**

### Rotating Structures

Figure 8 shows the rotating structure designed. The inset displays the vernier scale used to determine tip deflection when viewed under an SEM. Tip deflections recorded from the rotating structures vary between 1 and 2  $\mu\text{m}$ , corresponding to stresses between approximately 30 MPa and 50 MPa compressive. The wafer curvature measurements show stress in the same area of the wafer varying between 40 and 60 MPa compressive. On average, the values obtained from rotating structures are 20% lower than those recorded from the wafer curvature method.

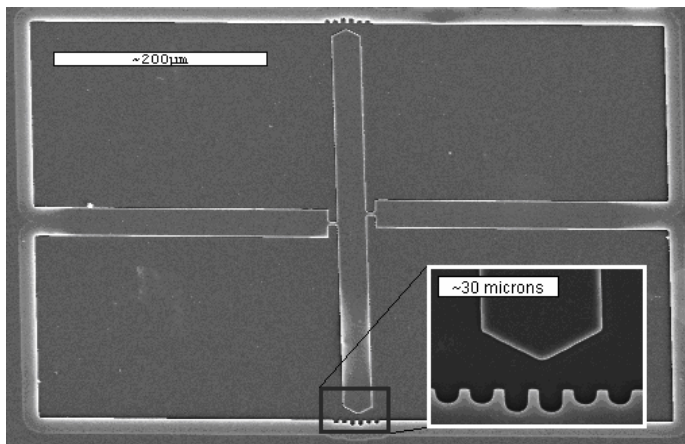


**FIGURE 8. SEM IMAGE OF THE ROTATING STRUCTURE DESIGNED FROM ZHANG ET AL. THE INSET SHOWS TIP DEFLECTION DUE TO STRESS AND ITS MEASUREMENT BY THE VERNIER SCALE.**

Although the two methods agree reasonable, it is difficult to measure low stresses with the rotating structures. The design selected from Zhang assumes a maximum residual stress of 200 MPa and was chosen based on average stress values from all wafers analyzed. Wafer A sees a maximum stress of approximately 90 MPa, however, and accurate determination of the small rotations obtained is difficult. Selecting rotating structure parameters designed to measure lower stress would improve resolution on wafer A.

### Method Comparison

Figure 7 compares compressive stress determined by the three microstructures to that of the wafer curvature method. The error bars on the x-axis specify the uncertainty of the wafer curvature measurements, while the error bars on the y-axis represent the detection limit of the microstructures. Error bars in the wafer curvature measurements are due to the 10 MPa stress increments resulting from software limitations as well as uncertainty in locating the test structures on the wafer curvature stress map in these stress ranges. In addition, other authors have recently indicated inherent limitations in the application of the Stoney equation for the determination of non-uniform stress across samples [14, 15]. All three mechanical methods give residual stress values comparable to the wafer curvature method. However, the stress determined from the rotating structures is about 20% lower than the other methods. The disagreement with the wafer curvature method of the lower two rotating structure stress values could be due to the effects of stiction. The indicators may not have been at their equilibrium stress states when stuck down.

## SUMMARY

Four mechanical methods for stress determination in thin films have been compared and stress variation across wafer processes as well as a single wafer has been determined. The wafer curvature method was used to obtain stress variation across thin polysilicon film processes including deposition and doping. All four methods were successfully used to determine residual stress variations across a single wafer. The wafer curvature and the doubly clamped vibrating and buckling beam methods all give comparable residual stress values for the wafer examined (40-90 MPa). However, the stress determined from rotating microstructures was 20% lower than values obtained from the wafer curvature method. The wafer curvature method has recently been shown to include errors when large stress variations occur across a single wafer, as was the case in the wafer examined. The local stress measuring structures compared show an important advantage in this situation where they can provide a more accurate stress map of the wafer with higher resolution [14, 15]. In all cases studied, while it was possible to produce tensile polysilicon films directly after deposition, all films were compressive after doping, even with additional annealing using RTP. This result differs from the results obtained by other authors who annealed their films using RTP prior to doping, resulting in tensile films [13].

## ACKNOWLEDGMENTS

This work was carried out in part through the use of the Massachusetts Institute of Technology Microsystem Technology Laboratories, and the University of Michigan Nanofabrication Facility. Dave Wilbur of Tufts University helped with SEM observations.

## REFERENCES

1. J. Singh, S. Chandra, and A. Chand, "Strain studies in LPCVD polysilicon for surface micromachined devices," *Sensors and Actuators a-Physical*, vol. 77, pp. 133-138, 1999.
2. D. G. Oei and S. L. McCarthy, "The Effect of Temperature and Pressure on Residual-Stress in Lpcvd Polysilicon Films," in *Smart Materials Fabrication and Materials for Micro-Electro-Mechanical Systems*, vol. 276, *Materials Research Society Symposium Proceedings*, 1992, pp. 85-90.
3. P. Krulevitch, G. C. Johnson, and R. T. Howe, "Stress and Microstructure in Phosphorus Doped Polycrystalline Silicon," in *Smart Materials Fabrication and Materials for Micro-Electro-Mechanical Systems*, vol. 276, *Materials Research Society Symposium Proceedings*, 1992, pp. 79-84.
4. B. P. Vandriehhuizen, J. F. L. Goosen, P. J. French, and R. F. Wolffenbuttel, "Comparison of Techniques for Measuring Both Compressive and Tensile-Stress in Thin-Films," *Sensors and Actuators a-Physical*, vol. 37-8, pp. 756-765, 1993.
5. L. Elbrecht, U. Storm, R. Catanescu and J. Binder, "Comparison of stress measurement techniques in surface micromachining," *Journal of Micromechanics and Microengineering*, vol. 7, pp. 151-154, 1997.
6. W. T. Thomson, M. D. Dahleh, *Theory of Vibrations with Applications*. New Jersey: Prentice Hall, 1998.
7. M.J. Madou, *Fundamentals of Microfabrication - The Science of Miniaturization*. 2<sup>nd</sup> Ed. Boca Raton: CRC Press, 2002.
8. H. Guckel, T. Randazzo, and D. W. Burns, "A Simple Technique for the Determination of Mechanical Strain in Thin-Films with Applications to Polysilicon," *Journal of Applied Physics*, vol. 57, pp. 1671-1675, 1985.
9. H. Guckel, Burns, H. A. , Tilmans, A. C. , DeRoo, D. W. , Rutigliano, C. R., "Mechanical properties of fine grained polysilicon the repeatability issue," *Solid-State Sensors and Actuators Workshop*, pp. 96-99, 1988.
10. X. Zhang, T. Y. Zhang, and Y. Zohar, "Measurements of residual stresses in thin films using micro-rotating-structures," *Thin Solid Films*, vol. 335, pp. 97-105, 1998.
11. P. J. French, "Polysilicon: a versatile material for microsystems," *Sensors and Actuators a-Physical*, vol. 99, pp. 3-12, 2002.
12. J. Yang, H. Kahn, A. Q. He, S. M. Phillips, and A. H. Heuer, "A new technique for producing large-area as-deposited zero-stress LPCVD polysilicon films: The MultiPoly process," *Journal of Microelectromechanical Systems*, vol. 9, pp. 485-494, 2000.
13. X. Zhang, T. Y. Zhang, M. Wong, and Y. Zohar, "Rapid thermal annealing of polysilicon thin films," *Journal of Microelectromechanical Systems*, vol. 7, pp. 356-364, 1998.
14. I. A. Blech, I. Blech, and M. Finot, "Determination of thin-film stresses on round substrates," *Journal of Applied Physics*, vol. 97, 2005.
15. K. S. Chen and K. S. Ou, "Modification of curvature-based thin-film residual stress measurement for MEMS applications," *Journal of Micromechanics and Microengineering*, vol. 12, pp. 917-924, 2002.